

1 **The nanostructural characterization of strawberry pectins in**
2 **pectate lyase or polygalacturonase silenced fruits elucidates their**
3 **role in softening**

4
5 **Sara Posé^{a1}, Andrew R. Kirby^b, Candelas Paniagua^a, Keith W. Waldron^b,**
6 **Victor J. Morris^b, Miguel A. Quesada^c, José A. Mercado^a**

7
8 ^aInstituto de Hortofruticultura Subtropical y Mediterránea “La Mayora” (IHSM-
9 UMA-CSIC), Departamento de Biología Vegetal, Universidad de Málaga, 29071,
10 Málaga, Spain

11 ^bInstitute of Food Research, Norwich Research Park, Colney, Norwich, NR4
12 7UA, UK

13 ^cDepartamento de Biología Vegetal, Universidad de Málaga, 29071, Málaga,
14 Spain

15
16 Author’s emails:

17 Sara Posé: S.Pose@leeds.ac.uk; Andrew R. Kirby: andrewkirby1966@gmail.com;

18 Candelas Paniagua: candelaspc@uma.es; Keith W. Waldron:

19 keith.waldron@ifr.ac.uk; Victor J. Morris: vic.morris@ifr.ac.uk; Miguel A.

20 Quesada: quefe@uma.es; José A. Mercado: mercado@uma.es

21
22 *Corresponding author:

23 José A. Mercado

24 Instituto de Horticultura Subtropical y Mediterránea “La Mayora”, IHSM-UMA-
25 CSIC, Departamento de Biología Vegetal, Universidad de Málaga, Campus
26 Teatinos s/n, 29071, Málaga, Spain

27 e-mail: mercado@uma.es; Fax: +34 952 13 20 00

28
29 ¹Present address: Centre for Plant Sciences, Faculty of Biological Sciences,
30 University of Leeds, Leeds, LS2 9JT, UK

31
32
33

34 **Abstract**

35 To ascertain the role of pectin disassembly in fruit softening, chelated- (CSP) and
36 sodium carbonate-soluble (SSP) pectins from plants with a pectate lyase, *Fap1C*,
37 or a polygalacturonase, *FaPG1*, downregulated by antisense transformation were
38 characterized at the nanostructural level. Fruits from transgenic plants were firmer
39 than the control, although *FaPG1* suppression had a greater effect on firmness.
40 Size exclusion chromatography showed that the average molecular masses of both
41 transgenic pectins were higher than that of the control. Atomic force microscopy
42 analysis of pectins confirmed the higher degree of polymerization as result of
43 pectinase silencing. The mean length values for CSP chains increased from 84 nm
44 in the control to 95.5 and 101 nm, in antisense *Fap1C* and antisense *FaPG1*
45 samples, respectively. Similarly, SSP polyuronides were longer in transgenic fruits
46 (61, 67.5 and 71 nm, in the control, antisense *Fap1C* and antisense *FaPG1*
47 samples, respectively). Transgenic pectins showed a more complex structure, with
48 a higher percentage of branched chains than the control, especially in the case of
49 *FaPG1* silenced fruits. Supramolecular pectin aggregates, supposedly formed by
50 homogalacturonan and rhamnogalacturonan I, were more frequently observed in
51 antisense *FaPG1* samples. The larger modifications in the nanostructure of pectins
52 in *FaPG1* silenced fruits when compared with antisense pectate lyase plants
53 correlate with the higher impact of polygalacturonase silencing on reducing
54 strawberry fruit softening.

55

56 **Keywords:** Atomic force microscopy, cell wall, *Fragaria* × *ananassa*, fruit
57 softening, homogalacturonan, pectins

58

59 Chemical compounds studied in this article

60 Galacturonan (PubChem CID: 445929)

61

62 **Abbreviations:** AFM, atomic force microscopy; APEL, antisense pectate lyase
63 plants; APG, antisense polygalacturonase plants; CDTA, cyclohexane-trans-1,2-
64 diamine tetraacetate; CSP, chelated soluble pectins; FTIR, Fourier transform
65 infrared spectroscopy; HGA, homogalacturonan; LN, number-average contour
66 length; LW, weight-average contour length; PDI, polydispersity index; PG,

67 polygalacturonase; PL, pectate lyase; RGI, rhamnogalacturonan I; SEC, size
68 exclusion chromatography; SSP, sodium carbonate soluble pectins

69

70 **1. Introduction**

71 Strawberry (*Fragaria × ananassa* Duch.) is the most economically important
72 edible soft fruit, which is characterized by its delicious flavour, intense colour,
73 soft texture and high nutritional value. Besides its economic importance, several
74 authors have proposed strawberry as a model for the study of the ripening process
75 in non-climacteric fruits (Posé et al., 2011). The fast softening of this fruit
76 determines its short post harvest life, which results in large losses due to over-
77 softening, bruising and subsequent fungal infections that generally are associated
78 with this process.

79 It is generally accepted that textural changes during ripening of fleshy fruits,
80 mainly a decrease in firmness, are caused by a reduction of cell to cell interaction
81 due to the dissolution of the middle lamella, a loosening of the primary cell wall
82 and a reduction in cell turgor (Goulao & Oliveira, 2008; Mercado, Pliego-Alfaro,
83 & Quesada, 2011). However, this last process is less well studied and is difficult
84 to separate from the previously mentioned changes in cell wall structure. Amongst
85 the different components that form the cell wall, polyuronides are the polymers
86 most likely to be extensively modified during ripening. This involves pectin
87 solubilization, i.e. an increase in the content of polyuronides loosely bound to the
88 wall, and depolymerization and the loss of neutral sugars from pectin side-chains
89 (Brummell, 2006; Goulao & Oliveira, 2008; Paniagua et al., 2014). These changes
90 are due to the coordinated action of cell wall modifying enzymes, such as
91 polygalacturonase (PG), pectate lyase (PL), pectin methyl esterase, β -
92 galactosidase or α -arabinofuranosidase, which are generally encoded by ripening-
93 related genes (Brummell & Harpster, 2001; Goulao & Oliveira, 2008; Mercado et
94 al., 2011). Amongst these enzymes PG (EC 3.2.1.15) has been the most studied
95 because certain fruits, e.g. tomato, peach or avocado, possess relatively high
96 levels of PG activity, which correlate with the rate of the softening process
97 (Brummell & Harpster, 2001). PG was also the first hydrolase to be examined
98 using transgenic methods in tomato (Sheehy, Kramer, & Hiatt, 1988; Smith et al.,
99 1988). However, the minor effect of PG silencing on tomato softening led to the

100 view that PG-mediated pectin disassembly during ripening makes only a small
101 contribution to fruit softening (Hadfield & Bennett, 1998; Brummell & Harpster,
102 2001). More recent studies on strawberry, apple and papaya have challenged this
103 hypothesis, suggesting a key role for pectin modifications in fruit softening
104 (Jiménez-Bermúdez et al., 2002; Quesada et al., 2009; Youssef et al., 2009;
105 Atkinson et al., 2012; Youssef et al., 2013; Fabi et al., 2014).

106 Ripening-specific genes encoding PG or PL (EC 4.2.2.2) enzymes have been
107 described in strawberry (Medina-Escobar, Cárdenas, Moyano, Caballero, &
108 Muñoz-Blanco, 1997; Villarreal, Rosli, Martínez, & Civello, 2008; Quesada et al.,
109 2009) and their roles in fruit softening evaluated by means of a functional
110 approach. In previous studies, our research group obtained transgenic strawberry
111 plants expressing antisense sequences of the *FapIC* gene, encoding a PL (Jiménez-
112 Bermúdez, et al. 2002; APEL lines) or the *FaPGI* gene, encoding a PG (Quesada
113 et al., 2009; APG lines). Ripe fruits from both transgenic genotypes were
114 significantly firmer than the wild type fruits. Based on their sequences, both genes
115 encode putative endo-pectinases with a common target, de-esterified
116 homogalacturonans (HGA), a major component of the primary cell wall and
117 middle lamella. However, the mechanisms of action of PL and PG are different as
118 are their optimum pH for enzymatic activity. Thus, PL cleaves HGA by β -
119 elimination in the presence of divalent cations with an *in vitro* optimal pH ~ 8
120 (Marín-Rodríguez, Orchard, & Seymour, 2002). The PG degrades HGA by
121 hydrolysis at acidic pH from 3.3 to 6.2 (Sénéchal, Wattier, Rustérucchi, & Pelloux,
122 2014). Chemical analysis of cell wall extracts from APEL and APG transgenic
123 fruits revealed that the silencing of both pectinases reduced middle lamella
124 dissolution and pectin solubilization (Santiago-Doménech et al., 2008; Posé et al.,
125 2013). Additionally, size exclusion chromatography results revealed higher
126 molecular masses for the polymers present in the pectin fractions from the
127 transgenic samples, which is consistent with a decreased depolymerization of
128 these polyuronides.

129 In general, cell wall hydrolases involved in fruit softening are encoded by large
130 gene families, within which a high degree of functional redundancy has been
131 observed (Vicente, Saladié, Rose, & Labavitch, 2007; Goulao & Oliveira, 2008).
132 It is unclear why a fruit invests energy on the simultaneous expression of PG and

133 PL enzymes acting on the same pectin domain, both having a key role on
134 strawberry softening. The enzymatic differences between PG and PL are not
135 enough to explain this redundancy. If these enzymes act on different targets within
136 the pectin matrix, the pectic chains of these two differently silenced transgenic
137 lines might show different degrees of polymerization and branching. This type of
138 structural modification can be characterized by atomic force microscopy (AFM) at
139 the nano-structural level (Morris, Kirby, & Gunning, 2010). This technique has
140 only recently been used to investigate pectin disassembly processes during fruit
141 ripening (Paniagua et al., 2014). The main goal of this research was to analyze at
142 the nano-structural level pectins from APG and APEL transgenic fruits to reveal
143 the different effect of each enzyme in the pectin matrix and its implications on the
144 mechanical properties of cell walls. Additional information has been obtained
145 through the use of Fourier transform infrared spectroscopy (FT-IR) and size
146 exclusion chromatography analysis (SEC). Based on previous studies, the present
147 research has focused the nanostructural characterization of pectins which are
148 ionically and covalently bound within the cell wall, since these fractions showed
149 the most extensive changes as a result of *FaPGI* or *FapIC* genes silencing
150 (Santiago-Doménech et al., 2008; Posé et al., 2013).

151

152 **2. Material and methods**

153

154 **2.1. Plant material**

155 Control, non-transformed, strawberry plants (*Fragaria × ananassa*, Duch., cv.
156 ‘Chandler’), transgenic antisense *FapIC* plants (line APEL39, described in
157 Jiménez-Bermúdez et al. (2002) and Santiago-Doménech et al. (2008)), and
158 antisense *FaPGI* plants (line APG29, described in Quesada et al. (2009) and Posé
159 et al. (2013)) were grown in a greenhouse under a natural temperature and
160 photoperiod regime. Transgenic ripe fruits showed a strong reduction in *FapIC* or
161 *FaPGI* mRNA levels, higher than 95%. The quality of the ripe fruits at harvest
162 was evaluated using only well-shaped fruits of uniform size and coloration, and
163 weight higher than 5 g. Color was estimated using a chroma meter Minolta CR-
164 400. Soluble solids were measured by using a refractometer Atago N1, and
165 firmness by using a hand-penetrometer (Effegi) with a cylindrical needle of 9.62

166 mm² area. pH was measured in juices extracted from fruits. A minimum of 25 ripe
167 fruits per line were evaluated. The fruits were harvested at the ripe stage, when
168 fully red, frozen in liquid N₂ and stored at -30°C until used.

169

170 **2.2. Cell wall extraction and pectin fractionation**

171 The cell walls were extracted from frozen ripe fruits following the protocol of
172 Redgwell, Melton & Brasch (1992) with some modifications, as described by
173 Santiago-Doménech et al. (2008). Briefly, 10-15 frozen fruits were ground to a
174 powder in liquid N₂ and 20 g were homogenised in 40 ml of PAW (phenol: acetic
175 acid: water, 2:1:1, w:v:v). The homogenate was centrifuged at 4000 g for 15min
176 and the supernatant filtered through Miracloth (Merck, Bioscience, UK). After
177 centrifugation, the pellet obtained was treated with 90% aqueous DMSO to
178 solubilise the starch. The extract was then centrifuged at 4000 g and the pellet
179 washed twice with distilled water. The water fraction was discarded, and the de-
180 starched pellet, the cell wall material (CWM), was lyophilised and weighed.

181 Pectin fractions were obtained as described by Santiago-Doménech et al.
182 (2008). CWM was washed overnight with deionised water, centrifuged at 6000 g
183 for 15 min and the pellet was sequentially extracted with 0.05 M trans-1,2-
184 diaminocyclohexane-N,N,N',N'-tetraacetic acid (CDTA) in 0.05 M sodium acetate
185 buffer, pH 6, followed by 0.1 M Na₂CO₃ containing 0.1% NaBH₄. CDTA
186 extracted polysaccharides (CSP fraction) are those held in the cell wall by Ca²⁺-
187 mediated crosslinks with the extracts likely to arise primarily from the middle
188 lamellae. Sodium carbonate solubilizes polysaccharides (SSP fraction) held in the
189 wall by ester linkages (Selvendran, 1985; Brummell, 2006) and likely to arise
190 mainly from the primary cell wall. Both pectin fractions were extensively dialyzed
191 and stored until required at -20°C as aqueous solutions, in order to avoid possible
192 aggregation, which might be induced on freeze-drying.

193 For neutral sugar analyses, samples from both pectin fractions were extracted
194 with 72% (w/w) sulphuric acid and derivatized to alditol acetates (Blakeney,
195 Harris, Henry & Stone, 1983). The alditol acetates were separated on a Restek
196 Rtx-225 column fitted to a Perkin-Elmer Autosystem XL gas chromatograph
197 equipped with a flame ionization detector.

198

199 **2.3. Infrared Spectroscopy**

200 Infrared spectra were recorded on a Jasco FT/IR-4100 (Spain) spectrometer
201 coupled to an Attenuated Total Reflectance (ATR) accessory (MIRacle ATR, PIKE
202 Technologies, USA) as previously described in Heredia-Guerrero et al. (2010).
203 Essentially, lyophilized samples were mounted on the ATR crystal and
204 compressed with a clamp and then their absorbance was monitored in the 4000-
205 600 cm^{-1} range at a resolution of 4 cm^{-1} and averaged over 25 scans. Spectra
206 Manager v.2 software (Jasco, Spain) was used to correct for both ATR effect and
207 atmospheric contributions from carbon dioxide and water vapor across the full
208 spectral range.

209

210 **2.4. Size exclusion chromatography**

211 The gel filtration chromatography measurements were performed as described
212 previously by Posé et al. (2013). Briefly, CSP and SSP pectin fractions were
213 loaded onto a 40 cm height x 10 mm internal diameter column filled with
214 Sepharose CL2B (Sigma–Aldrich Química SA, Spain). Gel medium was
215 equilibrated with 0.2M acetate buffer, pH 5, or 0.05 M TRIS–HCl buffer, pH 8.5,
216 for CSP and SSP samples, respectively. Samples were dissolved in the
217 corresponding equilibration buffer (6-8 mg ml^{-1}), loaded on the column (250 μl)
218 and eluted at a 14 ml h^{-1} flow rate. Column calibration of the void (V_0) and the
219 total (V_T) volumes were obtained by dextran blue and acetone, respectively.
220 Fractions (1 ml) were collected at a flow rate of 10 ml h^{-1} and assayed for uronic
221 acids (Filisetti-Cozzi & Carpita, 1991).

222

223 **2.5. Atomic Force Microscopy**

224 AFM samples were prepared following the protocol of Posé et al. (2012). Pectin
225 solutions were diluted to 1-5 $\mu\text{g ml}^{-1}$ in pure water or ammonium bicarbonate
226 buffer 10 mM, pH 8, and dissolved in a hot water bath for 30 min at 80°C. Then, 3
227 μl was pipetted onto freshly-cleaved mica (G250, Agar Scientific, UK). The mica
228 surface was dried over a heating block at 37-40°C for 20 min. The sample was
229 then inserted into the liquid cell of the microscope and visualized under tri-
230 distilled butanol. The mica was mounted in an AFM manufactured by ECS (East
231 Coast Scientific Limited, Cambridge, UK). Short tip AFM contact cantilevers

232 (Budget Sensors, Bulgaria) were used with a resonance frequency of 13 KHz and
233 a quoted force constant of 0.4 Nm^{-1} . The samples were scanned in contact mode at
234 a frequency of 2 Hz. Both topographical and error-signal mode images were
235 collected simultaneously. In excess of 100 images with an area $1 \mu\text{m}^2$ were
236 collected for each sample.

237

238 **2.6. AFM image analysis**

239 The ECS software (SPM 6.01, Cambridge, UK) plane fits and re-normalizes the
240 AFM images and it was used for chain height analysis (Kirby, Gunning, & Morris,
241 1996). The height of the chains was used to differentiate true branch points from
242 entangled chains (Adams, Kroon, Williamsom & Morris, 2003): overlapping
243 chains show a doubling of height at the crossover point. Further analyses were
244 applied offline. Initially, the original AFM files were converted to TIFF files using
245 Paint Shop Pro v. 5.00 software. Image contrast and stripe correction were
246 optimized using Gwyddion v2.32 software. Contour length measurements,
247 defined as total length including backbone and branches, were analyzed by
248 plotting the length of the chains with the freehand tool of ImageJ software
249 (Adams et al., 2003; Posé et al., 2012). Individual molecules were defined as
250 strands that were not entangled with, or overlapping other strands, that were long
251 enough to be exactly visualized, and which lay entirely within the scanned area
252 (Adams et al., 2003). In order to obtain reliable results, a minimum of 600 lengths
253 were measured per sample and the results represented as frequency histograms.
254 Number-average (L_N) and weight-average (L_W) contour lengths, as well as
255 polydispersity index (L_W/L_N , PDI) were calculated as described previously (Posé
256 et al., 2012). Additionally, other chain features were analyzed in order to
257 characterize the heterogeneous branch patterns of the chains; including number of
258 branching points per molecule and branch lengths.

259

260 **2.7. Statistical analysis**

261 The SPSS software (v. 19, IBM Corp. Route 100, Somers, NY) was used for
262 statistical analyses. Fruit characteristics were analyzed by ANOVA and mean
263 separation was done by Tukey test. The Levene test for homogeneity of variances
264 was performed prior to ANOVA. In the case of non-homogeneous variances, the

265 non-parametric Kruskal-Wallis test was used for multiple mean comparisons. In
266 AFM, at least three dozen images and more than 600 individual measurements
267 from each genotype and pectin sample were used to obtain the length distribution
268 representations and statistical parameters. The original data were compared with
269 the Kruskal-Wallis non-parametric median test. Original data were also
270 transformed by natural logarithm to obtain normal distributions, which were
271 compared by ANOVA. The Chi-square test was used to determine differences in
272 the branching of polymer chains and the percentage of micellar aggregates. All
273 statistical tests were performed at $P = 0.05$.

274

275

276 **3. Results**

277

278 **3.1. Characteristics of transgenic ripe fruits**

279 At ripening, fruits from both transgenic lines were firmer than control, being the
280 differences statistically significant (Table 1). However, the increase on fruit
281 firmness as result of *FaPGI* silencing was higher than the one achieved in
282 transgenic APEL fruits, 53% vs. 24% in APG and APEL fruits, respectively. Other
283 parameters related to overall fruit quality, i.e. soluble solids, pH and color, were
284 not modified or showed minor changes in the transgenic lines (Table 1). Fig. S1
285 (Supplementary data) shows the aspect of control and transgenic plants and fruits.

286

287 **3.2. FTIR analysis of fruit pectins**

288 ATR-FTIR spectra of CDTA (CSP) and sodium carbonate (SSP) soluble pectins
289 in control and transgenic lines are shown in Fig.1. Both fractions showed
290 absorption bands in the mid-infrared region, 1200-800 cm^{-1} , typical of
291 polyuronide samples rich in polygalacturonic acid. These bands are due to ring
292 vibrations overlapping with stretching vibration of the hydroxyl groups and the
293 glycosidic bond vibration, and can be used to identify polysaccharide mixtures
294 with different composition. When CSP fractions are compared with SSP, the later
295 showed an increase in the absorbance at 1075, 1047 and 953 cm^{-1} and a decrease
296 in the peak at 1100 cm^{-1} , suggesting different sugar compositions: the SSP pectin
297 is enriched in neutral sugars. No differences were detected in this region between

298 the control and transgenic samples, either for the CSP or SSP samples, indicating
299 that the pectinase silencing did not modify the neutral carbohydrate composition.
300 These results were confirmed by neutral sugar analysis using gas chromatography
301 (Table 2).

302 The relationship between peaks at 1737 cm^{-1} , assigned to C=O stretching
303 vibration of methyl esterified carboxylic groups, and 1625 cm^{-1} , corresponding to
304 the symmetrical stretching vibration of COO^- group, can be used to estimate the
305 degree of methyl esterification in the pectin samples (Manrique & Lajolo, 2002).
306 In the CSP samples, no differences between wild type and transgenic lines were
307 detected in the intensities of these absorption bands suggesting a similar degree of
308 methylation (Fig. 1A). As expected, the peak at 1737 cm^{-1} disappeared whereas
309 peaks at 1625 and 1415 cm^{-1} increased in SSP samples from control fruits, due to
310 the elimination of ester linkages during the alkaline extraction procedure (Fig.
311 1B). However, the SSP pectin fractions isolated from both transgenic genotypes
312 still maintained a strong absorption band at 1737 cm^{-1} (Fig. 1B), indicating the
313 presence of some ester bonds resistant to the mild alkaline conditions. Finally, the
314 low absorption at 1670 and 1588 cm^{-1} for amide bands, indicates an absence or
315 undetectable presence of protein in both pectin fractions.

316

317 **3.3. Size exclusion chromatography of bulk pectic polymers**

318 Pectin size modifications induced by the inhibition of *Fap1C* or *FaPG1* genes
319 were different. CDTA soluble pectins from the wild type fruits showed a profile
320 consisting of three peaks, which corresponded to three main groups of polymers
321 distributed throughout the eluted volume. The peak corresponding to the middle-
322 sized pectic polymers, eluting at 22 ml, was the most abundant (Fig. 2A). APG
323 samples showed a similar profile, but, in this case, an increased abundance of
324 larger polyuronides was observed in the first peak, eluting at 16 ml (Fig. 2B). By
325 contrast, APEL samples displayed a completely different profile with a main
326 prominent peak in the middle of the elution profile, showing a main pool of
327 middle-sized pectins (Fig. 2A). On the other hand, sodium carbonate soluble
328 fractions showed profiles with a main pool of low molecular size polymers that
329 eluted at 28 ml, close to the total volume (Fig. 2C, D). This peak was shifted to
330 the left in both transgenic samples when compared to the wild type control (Fig.

331 2C, D). This shift indicates a higher molecular mass in both of the transgenic
332 samples than in the wild type, revealing a lesser degree of depolymerisation in the
333 transgenic lines. Furthermore, both transgenic samples also included an extra peak
334 near the void volume that was not present in the wild type, this peak being more
335 prominent in the APEL samples (Fig. 2D).

336

337 **3.4. Nanostructural analysis of pectins by AFM**

338 The ability to analyze isolated polymer chains is the main advantage of the AFM
339 technique, when compared with bulk analysis by SEC, which allows unraveling of
340 a further level of pectin matrix complexity. AFM visualization not only allows
341 measurement of contour lengths from isolated chains, but also provides valuable
342 topographical information in order to differentiate between true branched points
343 and entangled chains. In general, AFM scanning of highly diluted strawberry
344 pectin extracts, in the range 10^{-6} g cm⁻³, showed isolated fibrous structures with
345 linear chains as the main feature and some aggregates (Supplementary Data, Fig.
346 S2A). True branched points have the same height than isolated chains (Fig. S2B,
347 profile 1). The aggregates were identified because they displayed higher heights
348 than isolated chains (Fig. S2B, profile 2). They were also present even at low
349 sample dilution when few isolated individual chains were present in the sample.
350 This suggests that aggregates are not formed by casual overlapping of individual
351 chains as result of the sample processing for AFM but are multi-polymer
352 complexes held together by intermolecular interactions. Interestingly, aggregates
353 often exhibited a defined structure having a core middle point of higher height
354 with emerging strands (Fig. S2). Similar structures have previously been observed
355 in other species and described as micellar like structures (Kirby, MacDougall, &
356 Morris, 2008; Morris, Gromer, & Kirby, 2009; Posé, Kirby, Mercado, Morris, &
357 Quesada, 2012). Figs. 3 and 4 show typical AFM images of CDTA and carbonate
358 extracted polysaccharides, respectively, isolated from ripe fruits from wild-type
359 and both transgenic lines. In general, CSP pectins were larger than SSP polymers.
360 A low proportion of branched chains and small aggregates were also present in the
361 samples. Qualitatively, AFM images showed more complex nano-structural
362 patterns in chains isolated from transgenic lines, both multi-branched molecules
363 and micellar aggregates were more abundant in these samples than in controls,

364 either in CSP (Fig. 3) or SSP samples (Fig. 4).

365 Contour lengths of several dozen isolated chains were recorded. Length
366 measurement from topographical AFM images provides enough information to
367 generate the characteristic position parameters L_N , L_W and the polydispersity
368 index (PDI) for the shape of contour length distributions (Round, MacDougall,
369 Ring, & Morris, 1997; Round, Rigby, MacDougall, Ring, & Morris, 2001).
370 Histograms for the length distribution for CSP samples were in the range 20-650
371 nm whilst SSP distribution ranged between 20 and 500 nm (Fig. 5). Both sets of
372 data were right-skewed and showed a good fitting to log-normal distributions
373 (Fig. 5). Table 3 shows the histogram parameters in CSP and SSP polymers from
374 control and transgenic lines. The median, as a more appropriate average for
375 asymmetrical distributions, was used to compare length distributions statistically.
376 In the case of CSP samples, antisense *FaPGI* fruits showed the highest L_N , L_W
377 and PDI values, with the median value of the length distributions being
378 statistically higher than the value obtained for the control. CSP samples from
379 antisense pectate lyase fruits showed an intermediate distribution of lengths
380 between APG and wild type. Polymers soluble in sodium carbonate were shorter
381 than those solubilized with CDTA, as previously described by Posé et al. (2012)
382 for ripe strawberry fruits. When the three genotypes were compared, the SSP
383 chains from the APG fruits were also significantly longer than the wild type, with
384 the APEL polymers showing an intermediate length between APG and wild type
385 (Table 3). The differences in CSP and SSP polymer lengths among the genotypes
386 studied can be easily visualized when the results are plotted as cumulative
387 frequencies (Fig. 5 D,H). Log-normal transformation of contour length data were
388 also applied to compare statistically wild type and transgenic samples, as
389 previously described by Posé et al. (2012), obtaining similar conclusions to those
390 described above.

391 In addition to changes in the length of the pectin chains, antisense silencing of
392 both pectinase genes also induced a modification of the chain branching pattern.
393 An increased percentage of branched molecules, as well as multi-branched
394 polymers, were observed in the two pectin fractions isolated from APG fruits
395 when compared to wild type (Table 4). In the APEL line, CSP polymers showed a
396 similar branching pattern than control, but SSP polymers displayed a higher

397 percentage of ramifications than the wild type, with the percentage of branching
398 molecules found to be slightly lower than observed in the APG samples (Table 4).
399 With regard to branch lengths, the CDTA fractions showed no significant
400 differences amongst the different lines. By contrast, the carbonate soluble pectin
401 fraction from the APG line had significantly longer branches than the APEL and
402 wild type lines (Table 4).

403 Finally, in the control samples the number of micellar-like aggregates per
404 scanned area was similar in the CSP and SSP pectin fractions (Fig. 6). By contrast,
405 in both transgenic samples, the presence of aggregates was higher in SSP samples
406 and these values were significantly higher than those found in the control SSP
407 fraction. The highest presence of aggregates was observed in both APG fractions.

408 In summary, the quantitative analysis of the AFM images indicates that the
409 silencing of both pectinases increases not only the length of the pectin molecules
410 but also their complexity, reflected in the higher percentage of branched
411 molecules and the increased number of supra-molecular complexes. Furthermore,
412 these differences were more conspicuous in pectin fractions from *FaPG1* silenced
413 fruits than in fractions from *FaplC* down-regulated fruits.

414

415

416 **5. Discussion**

417

418 The functional analyses of pectin degrading genes in fruits with extremely
419 different textural properties, such as strawberry and apple, have reopened the
420 debate about the role of pectin disassembly in fruit softening (Jiménez-Bermúdez
421 et al., 2002; Quesada et al., 2009; Atkinson et al., 2012). In an attempt to relate
422 disassembly at the nanostructural level with fruit softening, we have analyzed
423 pectin samples isolated from plants with a pectate lyase or a polygalacturonase
424 gene silenced, since both genotypes showed a significant increase in fruit
425 firmness. Additionally, we have already demonstrated in these genotypes that
426 pectins ionically bound to the cell wall, extracted with CDTA (CSP), and
427 covalently bound to the wall, sodium carbonate soluble pectins (SSP), displayed
428 extensive biochemical changes when compared with wild type fruits (Santiago-
429 Doménech et al., 2008; Posé et al., 2013).

430

431 **5.1. FTIR spectra and SEC analysis of transgenic pectin samples**

432 The mid-infrared region at 1200-800 cm^{-1} in FTIR spectra is used to identify
433 particular polysaccharides (Filippov, 1992; Largo-Gosens et al., 2014). In this
434 region, the CSP and SSP spectra from strawberry cell walls showed a maximum
435 peak at 1016 cm^{-1} , being indicative of pectin samples enriched in polygalacturonic
436 acid. However, different intensities in several bands within this region seen for the
437 CSP and SSP samples, suggest a higher proportion of neutral sugars in the SSP
438 polysaccharides (Coimbra, Barros, Barros, Rutledge & Delgadillo, 1998;
439 Kacuráková, Capek, Sasinková, Wellner & Ebringerová, 2000), which is in
440 accordance with the major presence of RGI in extracts solubilised by sodium
441 carbonate (Brummell, 2006). The silencing of both pectinase genes did not modify
442 the neutral sugar composition within the cell wall fractions. Similarly, the degree
443 of esterification in CSP pectins, estimated by the ratio of the peaks at 1745 and
444 1630 cm^{-1} (Manrique & Lajolo, 2002), was not altered in the transgenic
445 genotypes. The most striking difference between the control and the transgenic
446 samples was the presence of some ester bonds resistant to mild alkaline extraction
447 conditions in the transgenic SSP pectins, resulting in the presence of an absorption
448 band at about 1737 cm^{-1} despite the alkaline extraction. These ester bands could
449 be ascribed to phenolic esters, since the detailed observation of FTIR spectra of
450 transgenic SSP pectins exhibited a shoulder at 1720 cm^{-1} in the ester band (Fig.
451 1B) that is characteristic of aromatic esters (Séné, McCann, Wilson, & Grinter,
452 1994; Largo-Gosens et al., 2014). Alternatively, acetyl (Marry et al., 2006) and/or
453 borate (O'Neill et al., 2004) esters could also contribute to the ester band
454 fingerprint observed in the transgenic samples, but further research is required to
455 ascertain the exact nature of these ester bands

456 The bulk analysis of pectins by SEC revealed important differences in
457 polymer size distribution between *FaPGI* and *FaplC* transgenic cell walls.
458 *FaPGI* CSP samples displayed larger average molecular weights than the control
459 due to an increase in the relative abundance of polyuronides of large molecular
460 mass which eluted in the peak close to the void volume. However, *FaplC* down-
461 regulated fruits showed an increase on middle-size pectins. In the case of sodium
462 carbonate soluble pectins, both transgenics showed a similar displacement to the

463 left of the main peak, eluting in control fractions at 26 ml, and also an increased
464 amount of polyuronides, eluting at 10ml, that were not present in the control. This
465 peak, which corresponds to a molecular mass very close to the void volume of the
466 column, was significantly more abundant in APEL fruits. The absence of this peak
467 in control samples might indicate that these polyuronides were depolymerized
468 during ripening, leading to the two peaks that appeared at 14 and 17 ml in control
469 profile. Alternatively, the peak of large molecular mass that was absent in the
470 CDTA profile of APEL fruits might correspond to the strong peak that appears at
471 the same eluting volume in the SSP profile, since it has been suggested that
472 pectate lyase solubilizes subsets of strongly bound pectins (Santiago-Doménech et
473 al., 2008).

474

475 **5.2. AFM analysis of pectin samples revealed longer and more branched** 476 **polymers as a result of pectinase silencing**

477 Isolated pectin chains from the three genotypes were studied at the nano-structural
478 level by AFM. As observed previously in strawberry, peach and tomato fruits,
479 CSP pectin chains were larger than SSP ones (Round et al., 2001; Kirby et al.,
480 2008; Yang, Chen, An, & Lai, 2009; Posé et al., 2012). In general, number-
481 average (L_N) and weight-average (L_W) contour length values for both pectin
482 fractions were in the same range of those reported for equivalent pectin fractions
483 isolated from mature green tomato and sugar beet (Kirby et al., 2008; Round,
484 Rigby, MacDougall, & Morris, 2010). However, much longer pectin chains
485 (>1000 nm) have been observed in other fruits, i.e. peach (Yang et al., 2009),
486 jujube (Wang et al., 2012) and apricot (Chen et al., 2013). As regard the effect of
487 pectinase silencing on pectin nanostructure, AFM images illustrated the increase
488 in the size of CSP and SSP pectic chains from both transgenic fruits. The silencing
489 of *FapIC* gene increased L_N and L_W contour length values from CSP and SSP
490 samples in a similar magnitude, in the range of 9-20%, when compared with wild
491 type. Down-regulation of *FaPGI* had a stronger effect on pectin length, with L_N
492 and L_W , on average, 31 and 51% higher than the control values, respectively.
493 Interestingly, the increment on pectin length induced by PG silencing was slightly
494 higher in SSP than in CSP.

495 The number of carbohydrate residues as well as molecular mass of the pectic

496 structures visualized by AFM can be estimated from L_N and L_W values
497 considering a 3_1 helix structure with a pitch of 1.34 nm from fibre diffraction
498 analysis of polygalacturonic acid (Walkinshaw & Arnott, 1981). According to this
499 assumption, the degree of polymerization (DP) of control pectins was
500 approximately 231 and 161 residues for CSP and SSP fractions, respectively.
501 These values are slightly lower than those reported by Round et al. (2010) for
502 mature green tomato pectins extracted with sodium carbonate. The number of
503 residues was significantly increased in APG samples, 297 and 217 DP, for CSP
504 and SSP respectively, showing pectic chains from APEL fruits an intermediate
505 number of residues. It has been estimated that HG domains, obtained after fruit
506 pectin hydrolysis with 1N HCl, are about 72-117 DP (Thibault, Renard, Axelos,
507 Roger & Crépeau, 1993; Yapo, Lerouge, Thibault, & Ralet, 2007), whereas RG-I
508 isolated backbone is about 70-80 DP (Yapo et al., 2007). The chains depicted in
509 this study by AFM must account on more than one of those pectin domains. On
510 the other hand, although both the AFM and SEC studies support diminished pectin
511 degradation due to *FaPGI* or *FaplC* silencing, it is not possible to make a direct
512 comparison of the average molecular mass obtained for the pectic polymers
513 resolved in chromatography with those deduced from AFM images. AFM depicts
514 nanostructural details on isolated pectic chains while GFC monitors the volume of
515 the molecules in a complex mixture, based on hydrodynamic behaviour of
516 polymers through a porous gel matrix. Thus, longer and more branched pectin and
517 further micellar aggregations depicted by AFM could develop a more 'bulky'
518 pectin mixture, as is revealed by SEC.

519 In addition to pectin length, the branching patterns of the pectins were also
520 modified in the two transgenic genotypes analysed, especially in the case of
521 *FaPGI* silenced fruits. Both pectin fractions isolated from these fruits showed a
522 higher number of branches that were also longer than those observed in the
523 control in the case of SSP. By contrast, APEL lines only showed a higher
524 branching percentage than control in the sodium carbonate soluble fraction and
525 the branch length was not modified. Round et al. (1997) observed that almost 20%
526 of single polymers from sodium carbonate pectins from mature green tomato
527 visualized by AFM showed long branches, with approximately 30% of these
528 having more than one branch. Yang et al. (2009) suggested a relationship between

529 peach firmness and pectin nanostructure, since crisp cultivars showed longer and
530 more branched CSP and SSP polymers than soft fruits. In apricot and peach it has
531 also been observed that there is a reduction in branching during post harvest
532 storage of fruits (Yang, An, Feng, Li, & Lai, 2005; Liu et al., 2009). Recently,
533 AFM in pear fruits (Zdunek, Koziol, Pieczywek & Cybulska, 2014) also found a
534 higher branching index on CSP fractions in the firmer cultivar.

535 The physicochemical nature of linear chain branches is unclear. Neutral sugar
536 composition and linkage analyses suggested that the branches observed by AFM
537 in pectin chains do not correspond to neutral sugars but to polygalacturonic acid
538 attached to the pectin backbone via an undetermined branch point, with the
539 neutral sugars present as short branches undetected by AFM (Round et al., 2001).
540 This hypothesis was supported by experiments evaluating the effect of mild acid
541 hydrolysis on SSP pectins from unripe tomato (Round et al., 2010). This treatment
542 sequentially releases carbohydrate residues present in polyuronides at different
543 rates, Ara, Gal and Rha linkages being the most labile and GalA the most resistant
544 (Thibault et al., 1993). Round et al. (2010) observed that almost complete
545 hydrolysis of Ara, Gal and Rha had no significant effect on backbone and branch
546 length distributions in individual pectins visualized by AFM. The present results
547 indicate a higher branching when pectinases targeting HGA backbone are silenced
548 and they also support a polygalacturonic acid composition of the branches.

549 Transgenic fruits also displayed a higher number of micellar aggregates than
550 the control, especially in the case of *FaPGI* antisense fruits. Similar structures
551 have previously been described by AFM in tomato and sugar beet (Kirby et al.,
552 2008; Morris et al., 2009). It has been suggested that these complexes may contain
553 irreducible HGA linked to RG-I, since their size decreased upon acid hydrolysis in
554 parallel to neutral sugars lost (Round et al., 2010). As previously observed in
555 tomato pectins (Round et al., 2010), micellar aggregates from strawberry fruits
556 were often visualized with emerging strands with similar dimensions to isolated
557 chains. It is therefore probable that some of these HGA chains could be originally
558 linked to aggregates containing RG-I by bonds which would be broken during
559 ripening induced cell wall disassembly, and/or artificially during cell wall
560 chemical extraction or pectin fractionation. This interpretation of the aggregates
561 appearance is also in agreement with conformational studies performed in isolated

562 RG-I. The Rha units of the RG-I backbone, as well as the neutral sugar side
563 chains, confer a notable level of flexibility to this macromolecule, usually
564 resulting in the formation of very compact or sphere-like macromolecules in
565 contrast to the extended stiff rod-like conformation of HGA (Yapo, 2011).

566

567 **5.3. A hypothesis about the role of *FaPG1* and *Fap1C* on strawberry fruit** 568 **softening**

569 Fig. 7 shows a hypothetical mode of action of these two enzymes as deduced from
570 the results described above. Pectate lyase would act in restricted and more
571 localized microdomains in the primary cell wall reducing HGA backbone length
572 and the number of chain branches. This enzyme would play a minor role in the
573 degradation of middle lamella pectins extracted with CDTA. *FaPG1* protein, by
574 contrast, would have a wider spread and more pronounced activity than *Fap1C*
575 during strawberry ripening, degrading HGA backbone and reducing the number of
576 side-chains of middle lamella and primary cell wall polymers. Furthermore, this
577 protein also seems to act reducing the length of side-chains from pectin covalently
578 bound to the cell wall. The lesser effect of *Fap1C* downregulation on CDTA
579 pectins may be due to an esteric hindrance and/or restricted mobility of the *Fap1C*
580 enzyme within the primary cell wall, as has been suggested from
581 immunolocalization studies of pectate lyase proteins (Benítez-Burraco et al.,
582 2003). Differences in apoplastic pH could also contribute. During strawberry
583 ripening, pH decrease from 5 to 3 is observed (Moing et al., 2001), a pH value far
584 from the optimal pH for pectate lyase activity that is near to 8.5 (Sénéchal et al.,
585 2014). In addition to the effect on HGA, the silencing of both enzymes seems to
586 limit RG-I degradation, especially in the case of *FaPG1* plants. RG-I plays a
587 central function in the primary cell wall as a scaffold to which other pectic
588 polysaccharides, mainly HGA and RG-II, may be covalently attached to form the
589 pectin matrix which determines cell wall strength and mechanical properties
590 (Yapo, 2011). Our hypothesis is that the silencing of *FaPG1* or *Fap1C* not only
591 preserved HGA from degradation, as deduced from the more branched and longer
592 length of isolated chains, but would also reduce RG-I disassembly, reflected in a
593 higher density of aggregates in transgenic samples.

594

595 **6. Conclusions**

596 The silencing of polygalacturonase and pectate lyase genes reduced pectin
597 degradation during strawberry fruit softening, as confirmed both by SEC and
598 AFM analysis. The results obtained suggest that each pectinase acts on specific
599 pectin domains. In particular, polygalacturonase induced significant pectin
600 disassembly of polyuronides from both the middle lamella and primary cell wall,
601 whereas pectate lyase had a more limited effect, restricted mainly to pectins
602 covalently bound to the cell wall. These results correlate nicely with the firmer
603 phenotype of APG fruits when compared with fruits with down-regulated pectate
604 lyase. In summary, the fine structure elucidation of isolated pectins from
605 transgenic strawberry fruits revealed that, apart from the increased length, other
606 pectin features such as side chains distribution and aggregation status were
607 modified as result of pectinase silencing. It would be interesting to address
608 whether these effects are direct or side effects of pectinase action. Globally, these
609 structural features contribute to the reinforced mechanical strength of cell walls
610 for both transgenic fruits and support the load-bearing capacity of the pectin
611 matrix.

612

613

614 **Acknowledgements:** This work was supported by the Ministerio de Economía y
615 Competitividad of Spain and Feder European Union Funds (grant reference
616 AGL2011-24814). The research at IFR was supported through the BBSRC core
617 grant to the Institute. CP was supported with a FPI fellowship from the Spanish
618 Government (grant reference BES-2009-027985).

619

620

621 **References**

- 622 Adams, E. L., Kroon, P. A., Williamson, G., & Morris, V. J. (2003).
623 Characterisation of heterogeneous arabinoxylans by direct imaging of
624 individual molecules by atomic force microscopy. *Carbohydrate Research*,
625 338, 771-780.
- 626 Atkinson, R. G., Sutherland, P. W., Johnston, S. L., Gunaseelan, K., Hallett, I. C.,
627 Mitra, D., Brummell, D. A., Schröder, R., Johnston, J. W., & Schaffer, R. J.

628 (2012). Down-regulation of *POLYGALACTURONASE1* alters firmness, tensile
629 strength and water loss in apple (*Malus x domestica*) fruit. *BMC Plant Biology*,
630 *12*, 129-142.

631 Benítez-Burraco, A., Blanco-Portales, R., Redondo-Nevado, J., Bellido, M. L.,
632 Moyano, E., Caballero, J. L., & Muñoz-Blanco, J. (2003). Cloning and
633 characterization of two ripening-related strawberry (*Fragaria x ananassa* cv.
634 Chandler) pectate lyase genes. *Journal of Experimental Botany*, *54*, 633-645.

635 Blakeney, A. B., Harris, P. J., Henry, R. J., & Stone, B. A. (1983). A simple and
636 rapid preparation of alditol acetates for monosaccharide analysis.
637 *Carbohydrate Research*, *113*, 291-299.

638 Brummell, D. A. (2006). Cell wall disassembly in ripening fruit. *Functional Plant*
639 *Biology*, *33*, 103-119.

640 Brummell, D. A., & Harpster, M. H. (2001). Cell wall metabolism in fruit
641 softening and quality and its manipulation in transgenic plants. *Plant*
642 *Molecular Biology*, *47*, 311-340.

643 Chen, Y., Chen, F., Lai, S., Yang, H., Liu, H., Liu, K., Bu, G., & Deng, Y.
644 (2013). In vitro study of the interaction between pectinase and chelate-soluble
645 pectin in postharvest apricot fruits. *European Food Research and Technology*,
646 *217*, 1438-2377.

647 Coimbra, M. A., Barros, A., Barros, M., Rutledge, D. N., & Delgadillo, I. (1998).
648 Multivariate analysis of uronic acid and neutral sugars in whole pectic samples
649 by FT-IR spectroscopy. *Carbohydrate Polymers*, *37*, 241-248.

650 Fabi, J. P., García-Broetto, S., García Leme da Silva, S. L., Zhong, S., Lajolo, F.
651 M., & Oliveira do Nascimento, J. R. (2014). Analysis of papaya cell wall-
652 related genes during fruit ripening indicates a central role of
653 polygalacturonases during pulp softening. *PLOS One*, *9*, e105685.

654 Filisetti-Cozzi, T. M. C. C., & Carpita, N. C. (1991). Measurement of uronic acids
655 without interference from neutral sugars. *Analytical Biochemistry*, *197*, 157-
656 162.

657 Filippov, M. P. (1992). Practical infrared spectroscopy of pectic substances. *Food*
658 *Hydrocolloid*, *6*, 116-142.

- 659 Goulao, L. F., & Oliveira, C. M. (2008). Cell wall modification during fruit
660 ripening: when a fruit is not the fruit. *Trends in Food Science and Technology*,
661 *19*, 4-25.
- 662 Hadfield, K. A., & Bennett, A. B. (1998). Polygalacturonases: many genes in
663 search of a function. *Plant Physiology*, *117*, 337-43.
- 664 Heredia-Guerrero, J. A., San-Miguel, M. A., Sansom, M. S. P., Heredia, A., &
665 Benítez, J. J. (2010). Aleuritic (9, 10, 16-trihydroxypalmitic) acid self-
666 assembly on mica. *Physical Chemistry Chemical Physics*, *12*, 10423-10428.
- 667 Jiménez-Bermúdez, S., Redondo-Nevado, J., Muñoz-Blanco, J., Caballero, J. L.,
668 López-Aranda, J. M., Valpuesta, V., Pliego-Alfaro, F., Quesada, M. A., &
669 Mercado, J. A. (2002). Manipulation of strawberry fruit softening by antisense
670 expression of a pectate lyase gene. *Plant Physiology*, *128*, 751-759.
- 671 Kacuráková, M., Capek, P., Sasinková, V., Wellner, N., & Ebringerová, A. (2000).
672 FT-IR study of plant cell wall model compounds: Pectic polysaccharides and
673 hemicelluloses. *Carbohydrate Polymers*, *43*, 195-203.
- 674 Kirby, A. R., Gunning, A. P., & Morris, V. J. (1996). Imaging polysaccharides by
675 atomic force microscopy. *Biopolymers*, *38*, 355-366.
- 676 Kirby, A. R., MacDougall, A. J., & Morris, V. J. (2008). Atomic force microscopy
677 of tomato and sugar beet pectin molecules. *Carbohydrate Polymers*, *71*, 640-
678 647.
- 679 Largo-Gosens, A., Hernández-Altamirano, M., García-Calvo, L., Alonso-Simón,
680 A., Álvarez, J., & Acebes, J.L. (2014). Fourier transform mid infrared
681 spectroscopy applications for monitoring the structural plasticity of plant cell
682 walls. *Frontiers in Plant Science*, *5*, 303. doi: 10.3389/fpls.2014.00303
- 683 Liu, H., Chen, F., Yang, H., Yao, Y., Gong, X., Xin, Y., & Ding, C. (2009). Effect
684 of calcium treatment on nanostructure of chelate-soluble pectin and
685 physicochemical and textural properties of apricot fruits. *Food Research*
686 *International*, *42*, 1131-1140.
- 687 Manrique, G. D., & Lajolo, F. M. (2002). FT-IR spectroscopy as a tool for
688 measuring degree of methyl esterification in pectins isolated from ripening
689 papaya fruit. *Postharvest Biology and Technology*, *25*, 99-107.
- 690 Marín-Rodríguez, M. C., Orchard, J., & Seymour, G. B. (2002). Pectate lyase, cell
691 wall degradation and fruit softening. *Journal of Experimental Botany*, *53*,

692 2115–2119.

693 Marry, M., Roberts, K., Jopson, S. J., Huxham, M., Jarvis, M. C., Corsar, J.,
694 Robertson, E., & McCann, M. C. (2006). Cell-cell adhesion in fresh sugar-beet
695 root parenchyma requires both pectin esters and calcium cross-links.
696 *Physiologia Plantarum*, *126*, 243-256.

697 Medina-Escobar, N., Cárdenas, J., Moyano, E., Caballero, J. L., & Muñoz-Blanco,
698 J. (1997). Cloning, molecular characterization and expression pattern of a
699 strawberry ripening-specific cDNA with sequence homology to pectate lyase
700 from higher plants. *Plant Molecular Biology*, *34*, 867-877.

701 Mercado, J. A., Pliego-Alfaro, F., & Quesada, M. A. (2011). Fruit shelf life and
702 potential for its genetic improvement. In M. A. Jenks, & P. J. Bebeli (Eds.),
703 *Breeding for Fruit Quality* (pp. 81-104). Oxford: John Wiley & Sons, Inc..

704 Moing, A., Renaud, C., Gaudillère, M., Raymond, P., Roudeillac, P., & Denoyes-
705 Rothan, B. (2001). Biochemical changes during fruit development of four
706 strawberry cultivars. *Journal of the American Society for Horticultural*
707 *Science*, *126*, 394-403.

708 Morris, V. J., Gromer, A., & Kirby, A. R. (2009). Architecture of intracellular
709 networks in plant matrices. *Structural Chemistry*, *20*, 255-261.

710 Morris, V. J., Kirby, A. R., & Gunning, A. P. (2010). *Atomic force microscopy for*
711 *biologists*. London: Imperial College Press.

712 O'Neill, M. A., Ishii, T., Albersheim, P., & Darvill, A. G. (2004).
713 Rhamnogalacturonan II: structure and function of a borate cross-linked cell
714 wall pectic polysaccharide. *Annual Review of Plant Biology*, *55*, 109-139.

715 Paniagua, C., Posé, S., Morris, V. J., Kirby, A. R., Quesada, M. A., & Mercado, J.
716 A. (2014). Fruit softening and pectin disassembly: an overview of
717 nanostructural pectin modifications assessed by atomic force microscopy.
718 *Annals of Botany*, *114*, 1375-1383.

719 Posé, S., García-Gago, J. A., Santiago-Doménech, N., Pliego-Alfaro, F., Quesada,
720 M. A., & Mercado, J. A. (2011). Strawberry fruit softening: role of cell wall
721 disassembly and its manipulation in transgenic plants. *Genes, Genomes and*
722 *Genomics*, *5*, 40-48.

723 Posé, S., Kirby, A. R., Mercado, J. A., Morris, V. J., & Quesada, M. A. (2012).
724 Structural characterization of cell wall pectin fractions in ripe strawberry fruits
725 using AFM. *Carbohydrate Polymers*, 88, 882-890.

726 Posé, S., Paniagua, C., Cifuentes, M., Blanco-Portales, R., Quesada, M. A., &
727 Mercado, J. A. (2013). Insights into the effects of polygalacturonase *FaPGI*
728 gene silencing on pectin matrix disassembly, enhanced tissue integrity, and
729 firmness in ripe strawberry fruits. *Journal of Experimental Botany*, 64, 3803-
730 3815.

731 Quesada, M. A., Blanco-Portales, R., Posé, S., García-Gago, J. A., Jiménez-
732 Bermúdez, S., Muñoz-Serrano, A., Caballero, J. L., Pliego-Alfaro, F.,
733 Mercado, J. A., & Muñoz-Blanco, J. (2009). Antisense down-regulation of the
734 *FaPGI* gene reveals an unexpected central role for polygalacturonase in
735 strawberry fruit softening. *Plant Physiology*, 150, 1022-1032.

736 Redgwell, R. J., Melton, L. D., & Brasch, D. J. (1992). Cell-wall dissolution in
737 ripening kiwifruit (*Actinidia deliciosa*). Solubilisation of the pectic polymers.
738 *Plant Physiology*, 98, 71-81.

739 Round, A. N., MacDougall, A. J., Ring, S. G., & Morris, V. J. (1997). Unexpected
740 branching in pectin observed by atomic force microscopy. *Carbohydrate*
741 *Research*, 303, 251-253.

742 Round, A. N., Rigby, N. M., MacDougall, A. J., Ring, S. G., & Morris, V. J.
743 (2001). Investigating the nature of branching in pectin by atomic force
744 microscopy and carbohydrate analysis. *Carbohydrate Research*, 331, 337-342.

745 Round, A. N., Rigby, N. M., MacDougall, A. J., & Morris, V. J. (2010). A new
746 view of pectin structure revealed by acid hydrolysis and atomic force
747 microscopy. *Carbohydrate Research*, 345, 487-497.

748 Santiago-Doménech, N., Jiménez-Bermúdez, S., Matas, A. J., Rose, J. K. C.,
749 Muñoz-Blanco, J., Mercado, J. A., & Quesada, M. A. (2008). Antisense
750 inhibition of a pectate lyase gene supports a role for pectin depolymerization in
751 strawberry fruit softening. *Journal of Experimental Botany*, 59, 2769-2779.

752 Selvendran, R. R. (1985). Developments in the chemistry and biochemistry of
753 pectic and hemicellulosic polymers. *Journal of Cell Science, Supplement 2*, 51-
754 88.

755 Séné, C. F. B., McCann, M. C., Wilson, R. H., & Grinter, R. (1994). Fourier-
756 transform Raman and Fourier-transform infrared spectroscopy (an
757 investigation of five higher plant cell walls and their components). *Plant*
758 *Physiology*, 106, 1623-1631.

759 Sénéchal, F., Wattier, C., Rustérucci, C., & Pelloux, J. (2014).
760 Homogalacturonan-modifying enzymes: structure, expression, and roles in
761 plants. *Journal of Experimental Botany* DOI:10.1093/jxb/eru272

762 Sheehy, R. E., Kramer, M. K., & Hiatt, W. R. (1988). Reduction of
763 polygalacturonase activity in tomato fruit by antisense RNA. *Proceedings of*
764 *the National Academy of Sciences USA*, 85, 8805-8809.

765 Smith, C. J. S., Watson, C. F., Ray, J., Bird, C. R., Morris, P. C., Schuch, W., &
766 Grierson, D. (1988). Antisense RNA inhibition of polygalacturonase gene
767 expression in transgenic tomatoes. *Nature*, 334, 724-726.

768 Thibault, J.-F., Renard, C. M. G. C., Axelos, M. A. V., Roger, P., & Crépeau, M.-J.
769 (1993). Studies of the length of homogalacturonic regions in pectins by acid
770 hydrolysis. *Carbohydrate Research*, 238, 271-286.

771 Vicente, A. R., Saladié, M., Rose, J. K. C., & Labavitch, J. M. (2007). The linkage
772 between cell wall metabolism and fruit softening: looking to the future. *Journal*
773 *of the Science of Food and Agriculture*, 87, 1435–1448.

774 Villarreal, N. M., Rosli, H. G., Martínez, G. A., & Civello, P. M. (2008).
775 Polygalacturonase activity and expression of related genes during ripening of
776 strawberry cultivars with contrasting fruit firmness. *Postharvest Biology and*
777 *Technology*, 47, 141-150.

778 Walkinshaw, M. D., & Arnott, S. (1981). Conformations and interactions of
779 pectins. I. X-ray diffraction analyses of sodium pectate in neutral and acidified
780 forms. *Journal of Molecular Biology*, 153, 1055-1074.

781 Wang, H., Chen, F., Yang, H., Chen, Y., Zhang, L., & An, H. (2012). Effects of
782 ripening stage and cultivar on physicochemical properties and pectin
783 nanostructure of jujubes. *Carbohydrate Polymers*, 89, 1180-1188.

784 Yang, H., An, H., Feng, G., Li, Y., & Lai, S. (2005). Atomic force microscopy of
785 the water-soluble pectin of peaches during storage. *European Food Research*
786 *and Technology*, 220, 587-591.

787 Yang, H., Chen, F., An, H., & Lai, S. (2009). Comparative studies on

788 nanostructures of three kinds of pectins in two peach cultivars using atomic
789 force microscopy. *Postharvest Biology and Technology*, 51, 391-398.

790 Yapo, B. M., Lerouge, P., Thibault, J.-F., & Ralet, M.-C. (2007). Pectins from
791 citrus peel cell walls contain homogalacturonans homogeneous with respect to
792 molar mass, rhamnogalacturonan I and rhamnogalacturonan II. *Carbohydrate*
793 *Polymers*, 69, 426-435.

794 Yapo, B. M. (2011). Pectic substances: from simple pectic polysaccharides to
795 complex pectins - A new hypothetical model. *Carbohydrate Polymers*, 86, 373-
796 385.

797 Youssef, S. M., Jiménez-Bermúdez, S., Bellido, M. L., Martín-Pizarro, C.,
798 Barceló, M., Abdal-Aziz, S. A., Caballero, J. L., López-Aranda, J. M., Pliego-
799 Alfaro, F., Muñoz, J., Quesada, M. A., & Mercado, J. A. (2009). Fruit yield and
800 quality of strawberry plants transformed with a fruit specific strawberry pectate
801 lyase gene. *Scientia Horticulturae*, 119, 120-125.

802 Youssef, S. M., Amaya, I., López-Aranda, J. M., Sesmero, R., Valpuesta, V.,
803 Casadoro, G., Blanco-Portales, R., Pliego-Alfaro, F., Quesada, & M. A.,
804 Mercado, J, A. (2013). Effect of simultaneous down-regulation of pectate lyase
805 and endo- β -1,4-glucanase genes on strawberry fruit softening. *Molecular*
806 *Breeding*, 31, 313-322.

807 Zdunek, A., Koziol, A., Pieczywek, P.M., & Cybulska, J. (2014). Evaluation of the
808 nanostructure of pectin, hemicellulose and cellulose in the cell walls of pears of
809 different texture and firmness. *Food and Bioprocess Technology*, 7, 3525-3535.

810

Table 1. Characteristics of transgenic fruits with *Fap1C* (APEL) or *FaPG1* (APG) genes down-regulated by antisense transformation. Fruits were harvested at the stage of full ripeness. Data correspond to mean±SD of a minimum of 25 fruits per line. Means with different letters indicate significant differences by Tukey (soluble solids, pH, color a) or Kruskal-Wallis (firmness, color L and b) tests, both at $P=0.05$.

	Control	APEL	APG
Firmness (N)	3.3±0.5c	4.1±0.6b	5.0±0.8a
pH	3.5±0.1a	3.4±0.02a	3.5±0.1a
Soluble solids (°Brix)	7.7±1.6a	8.3±1.4a	7.6±1.5a
Color			
L	37.3±2.7a	39.9±6.4a	35.7±3.0b
a	37.4±4.5b	40.1±3.4a	36.5±3.7b
b	20.2±3.3b	25.2±7.0a	19.2±3.6b

Table 2. Neutral sugar content in CDTA (CSP) and sodium carbonate (SSP) soluble pectins from fruits with *FapIC* (APEL) or *FaPGI* (APG) genes down-regulated. Values correspond to mean±SD of three independent replicates.

		Neutral sugar (mol%)						
		Rha	Fuc	Ara	Xyl	Man	Gal	Glc
CSP	Control	7.2±0.03	1.3±0.5	33.7±0.2	4.1±0.2	3.7±0.8	47.9±1.5	2.0±0.7
	APEL	7.6±0.5	1.2±0.1	32.3±1.2	4.4±0.1	4.0±0.5	48.2±1.7	2.4±0.3
	APG	7.3±1.1	1.1±0.3	33.7±0.1	3.5±0.9	4.8±1.8	47.6±1.7	3.5±0.9
SSP	Control	4.8±0.2	0.6±0.02	27.7±0.3	2.7±0.1	1.5±0.2	61.7±0.1	1.0±0.1
	APEL	5.0±0.03	0.5±0.01	28.5±0.3	2.5±0.1	1.4±0.2	61.3±0.02	0.8±0.04
	APG	4.4±0.6	0.4±0.1	28.7±0.1	2.3±0.2	1.1±0.2	62.4±1.2	0.7±0.1

Table 3. AFM characterization of pectins chains in fruits with *Fap1C* (APEL) or *FaPG1* (APG) genes down-regulated. Pectins were extracted from ripe strawberry fruits from control and transgenic lines and analysed by AFM in contact mode. Descriptors of contour length distributions (number-average (L_N), weight-average (L_W) and polydispersity index (PDI)) of CDTA (CSP) and sodium carbonate (SSP) soluble pectins obtained from AFM images. ME corresponds to the median value of original data. Within each pectin fraction, median values followed by different letters are significantly different by non-parametric median test at $P=0.05$. N = 710, 734 and 660 for Control, APEL and APG CDTA samples, and N = 673, 608 and 527 for Na_2CO_3 samples, respectively.

		L_N (nm)	L_W (nm)	PDI	ME (nm)
CSP	Control	103.2	147.1	1.42	84.0 b
	APEL	112.4	164.3	1.46	93.5 a
	APG	132.8	211.7	1.59	101.0 a
SSP	Control	72.3	97.7	1.35	61.0 b
	APEL	80.4	117.7	1.46	67.5 ab
	APG	96.9	156.2	1.61	71.0 a

Table 4. AFM characterization of pectin branches in fruits with *Fap1C* (APEL) or *FaPG1* (APG) genes down-regulated. Pectins were extracted from ripe strawberry fruits from control and transgenic lines and analysed by AFM in contact mode. Branch length distribution parameters (number-average (L_N), weight-average (L_W) and polydispersity index (PDI)) and branching pattern of CDTA (CSP) and sodium carbonate (SSP) soluble pectins obtained from AFM samples. ME corresponds to the median value of original data. Branching was defined as the percentage of branched molecules per total number of molecules. Multibranching was defined as the percentage of polymers with more than one branch per branched molecules. Within each pectin fraction, median values followed by different letters are significantly different by the non-parametric median test at $P=0.05$. Chi-square test was used for branching percentages. $N = 52, 53$ and 118 for Control, APEL and APG CDTA samples, and $N = 63, 87$ and 94 for Control, APEL and APG for Na_2CO_3 samples.

		Branch parameters				Branching pattern (%)	
		L_N (nm)	L_W (nm)	PDI	ME (nm)	Branching	Multibranching
CSP	Control	57.8	84.3	1.46	48.0a	7.3b	1.9b
	APEL	63.4	87.0	1.37	54.0a	7.2b	5.7b
	APG	63.8	86.6	1.36	51.0a	17.9a	21.2a
SSP	Control	34.1	43.5	1.27	29.5b	9.4b	4.8b
	APEL	33.3	47.5	1.44	28.0b	14.3a	13.8a
	APG	51.7	67.9	1.31	41.0a	17.9a	20.2a

Figures

Figure 1. ATR-FTIR spectra of CDTA (A) and sodium carbonate-soluble (B) pectin fractions in the 2000-800 cm^{-1} region. Pectins were extracted from ripe fruits of Control, *Fap1C* (APEL) and *FaPG1* (APG) antisense transgenic lines (dashed, grey and black lines respectively). Inlet in Fig. 1-B shows detailed peaks of esterified ($\sim 1737 \text{ cm}^{-1}$) and deesterified ($\sim 1625 \text{ cm}^{-1}$) carboxyl groups, displaying both transgenic lines a recalcitrant pool of esterified residues.

Figure 2. Chromatographic elution profiles of polyuronides extractable by CDTA (A, B) and sodium carbonate (C, D) from cell walls of wild-type, antisense *Fap1C* (APEL; figures A,C) and antisense *FaPG1* (APG; figures B,D) ripe fruits. Profiles were obtained by size exclusion chromatography on Sepharose CL-2B. Columns were calibrated by dextran blue and acetone for void volume (V_0) and total volume (V_T), respectively. Fractions were assayed for uronic acid and expressed as relative optical density (OD) at 515 nm. The results show the average profile of at least two independent chromatographic assays per sample.

Figure 3. Typical AFM images, in topographical mode, of CSP-pectin samples from cell walls of wild-type (A), antisense *Fap1C* (B) and antisense *FaPG1* (C) ripe fruits. Images 1-6 correspond to zoomed areas to show unbranched isolated chains (1,3), branched isolated molecules (5) and micellar aggregates (2,4,6). Scan size: 1 μm (A-C) and 250 nm (1-6).

Figure 4. Typical AFM images of SSP-pectin samples from cell walls of wild-type (A), antisense *Fap1C* (B) and antisense *FaPG1* (C) ripe fruits. Images 1-6 correspond to zoomed areas to show unbranched isolated chains (1), branched molecules (3,4,5) and micellar aggregates (2,6). Scan size: 1 μm (A-C) and 250 nm (1-6).

Figure 5. Contour length distribution of CDTA (CSP) and sodium carbonate (SSP) soluble polymers isolated from fruit cell walls of control (A, E), antisense *Fap1C* (APEL; figures B, F) and antisense *FaPG1* (APG; figures C, G) ripe fruits. Bars represent relative frequencies of the observed data. (D, H) Cumulative

frequencies for CSP (D) and SSP (H) fractions, normalized to the maximum frequency value.

Figure 6. Average number of micellar aggregates in CDTA (CSP) and sodium carbonate (SSP) soluble pectin samples isolated from cell walls of control, antisense *FapIC* (APEL) and antisense *FaPGI* (APG) ripe fruits. For each pectin sample, bars with different letters indicate significant differences by Tukey test at $P=0.05$.

Figure 7. Schematic representation of a hypothetical mode of action for pectate lyase and polygalacturonase on CDTA and sodium carbonate pectin chains during strawberry ripening based on AFM analysis of antisense *FapIC* (APEL) and *FaPGI* (APG) ripe fruits. Length of pectin chains and branches, as well as the number of branches per chain are drawing at scale. Scissors indicate putative points of cutting for both enzymes. Pectate lyase would reduce HGA backbone length and the number of chain branches. This enzyme might play a minor role in the degradation of middle lamella pectins extracted with CDTA. Polygalacturonase has a more pronounced activity during strawberry ripening, degrading HGA backbone, and reducing the number of side-chains of pectins from both polyuronide fractions, as well as the length of sodium carbonate pectin side-chains.

Supplementary data

Supplementary Fig. S1. Aspect of plants and fruits from control and antisense *Fap1C* (Apel39) and antisense *FaPG1* (APG29) genotypes.

Supplementary Fig. S2. (A) Representative image of CDTA pectins from strawberry ripe fruit obtained by AFM in contact mode. Branched pectin chains and micellar aggregates with emerging strands can be observed in the image. (B) Height profiles, showing the heights in a true branch point (black arrow) of a polymer chain (profile 1) and micellar aggregates (profile 2) with emerging strands of same height than isolated chains (grey arrow) and higher height at the core area (arrowhead).

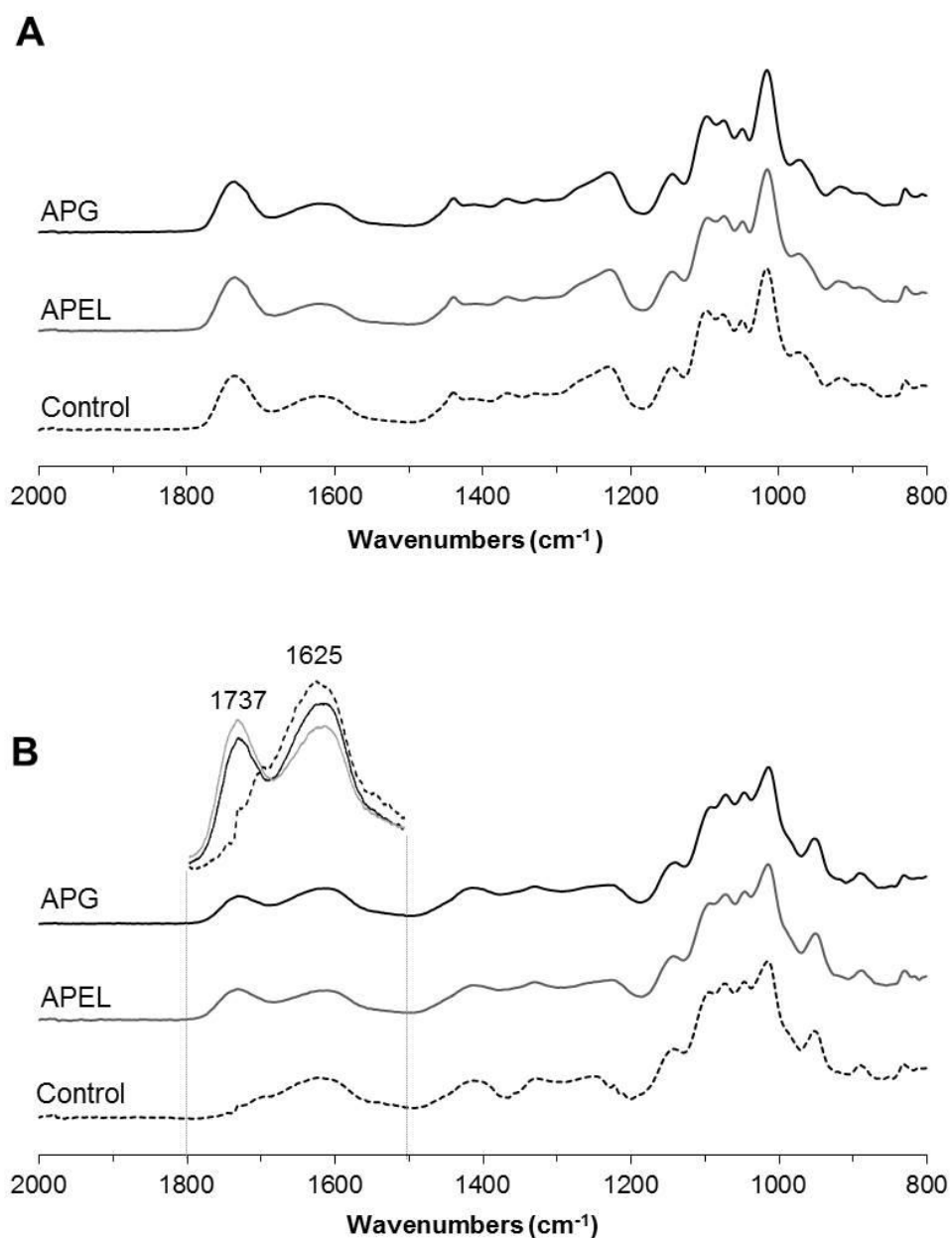


Figure 1. ATR-FTIR spectra of CDTA (A) and sodium carbonate-soluble (B) pectin fractions in the 2000-800 cm⁻¹ region. Pectins were extracted from ripe fruits of Control, *Fap1C* (APEL) and *FaPG1* (APG) antisense transgenic lines (dashed, grey and black lines respectively). Inlet in Fig. 1-B shows detailed peaks of esterified (~1737 cm⁻¹) and deesterified (~1625 cm⁻¹) carboxyl groups, displaying both transgenic lines a recalcitrant pool of esterified residues.

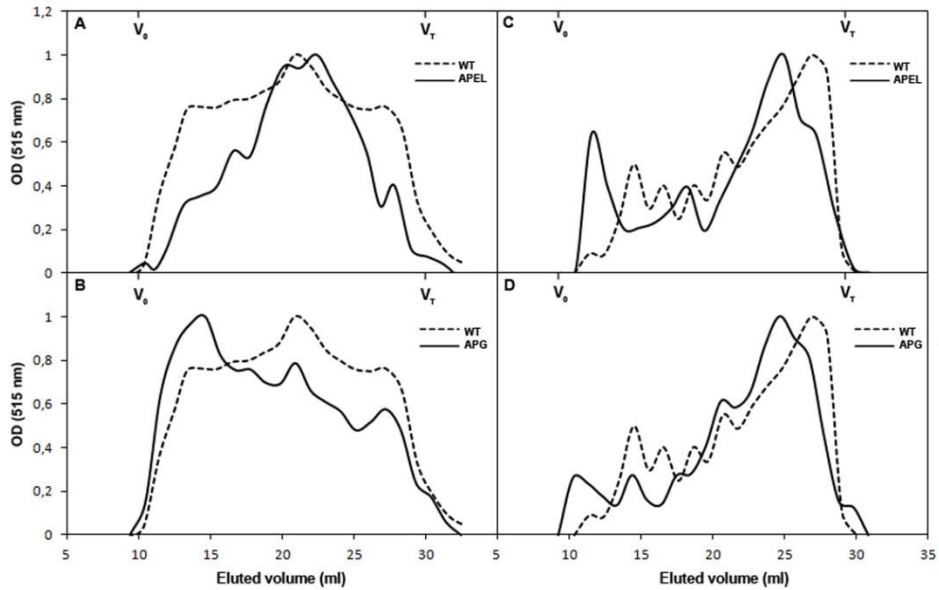


Figure 2. Chromatographic elution profiles of polyuronides extractable by CDTA (A, B) and sodium carbonate (C, D) from cell walls of wild-type, antisense *FapIC* (APEL; figures A,C) and antisense *FaPG1* (APG; figures B,D) ripe fruits. Profiles were obtained by size exclusion chromatography on Sepharose CL-2B. Columns were calibrated by dextran blue and acetone for void volume (V_0) and total volume (V_T), respectively. Fractions were assayed for uronic acid and expressed as relative optical density (OD) at 515 nm. The results show the average profile of at least two independent chromatographic assays per sample.

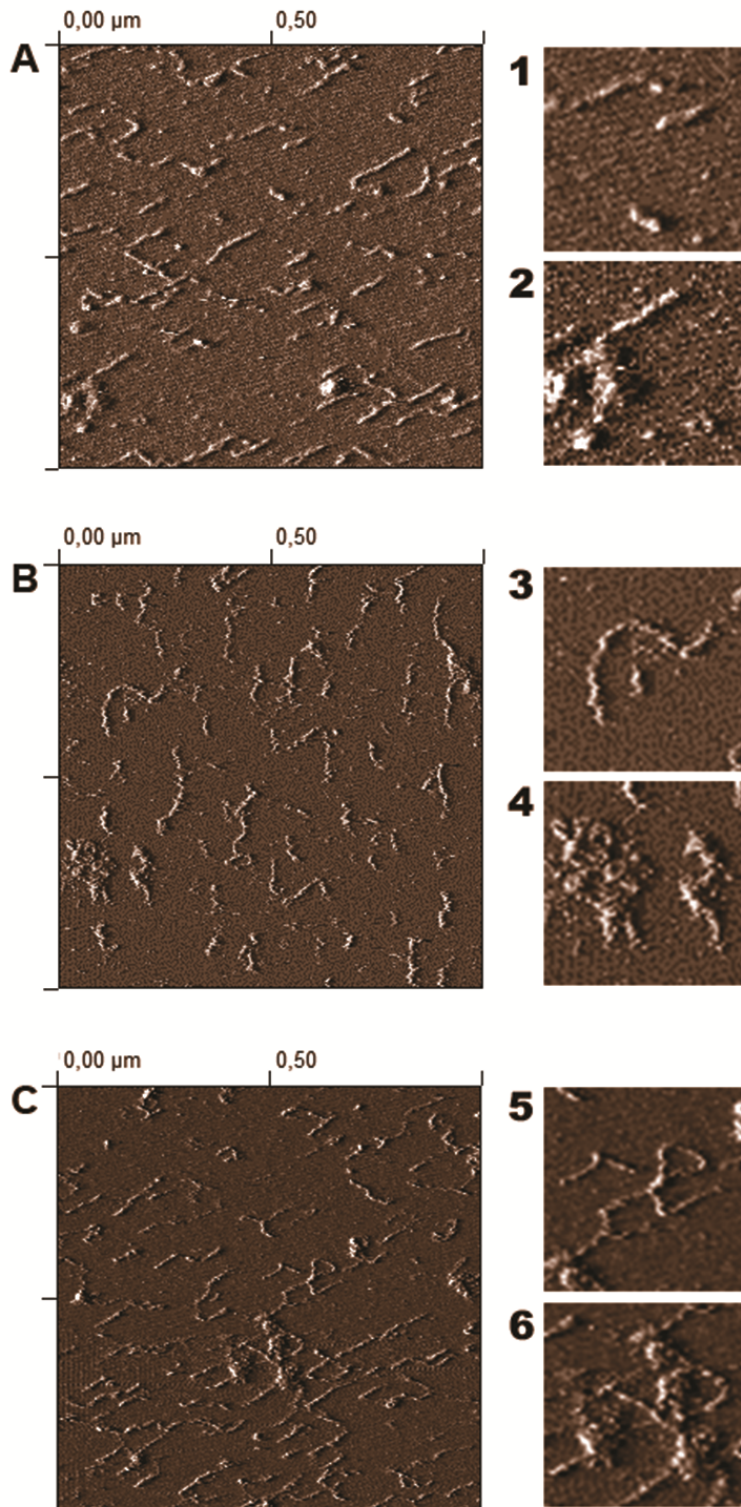


Figure 3. Typical AFM images, in topographical mode, of CSP-pectin samples from cell walls of wild-type (A), antisense *FapIC* (B) and antisense *FaPG1* (C) ripe fruits. Images 1-6 correspond to zoomed areas to show unbranched isolated chains (1,3), branched isolated molecules (5) and micellar aggregates (2,4,6). Scan size: 1 μm (A-C) and 250 nm (1-6).

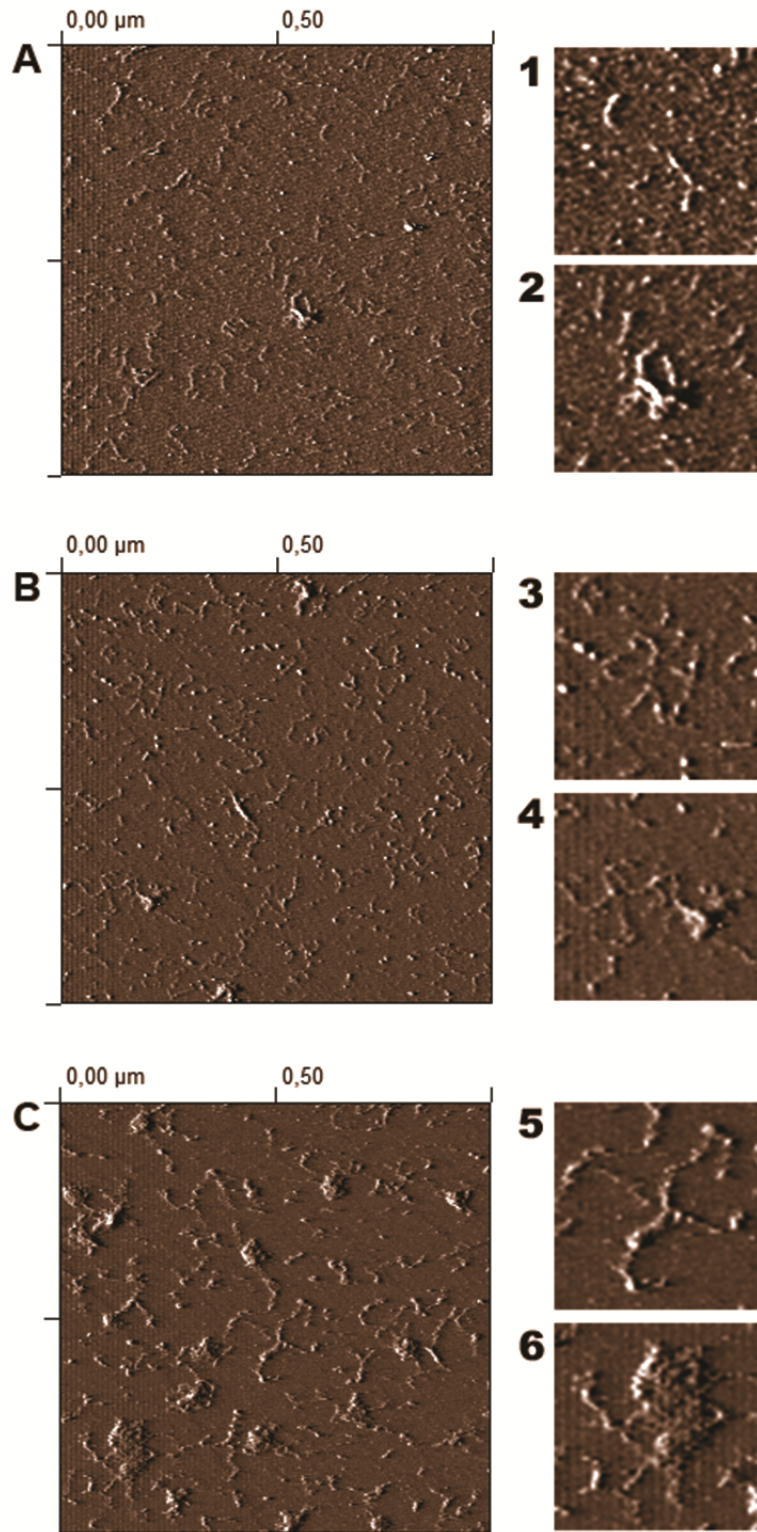


Figure 4. Typical AFM images of SSP-pectin samples from cell walls of wild-type (A), antisense FapIC (B) and antisense FaPG1 (C) ripe fruits. Images 1-6 correspond to zoomed areas to show unbranched isolated chains (1), branched molecules (3,4,5) and micellar aggregates (2,6). Scan size: 1 μm (A-C) and 250 nm (1-6).

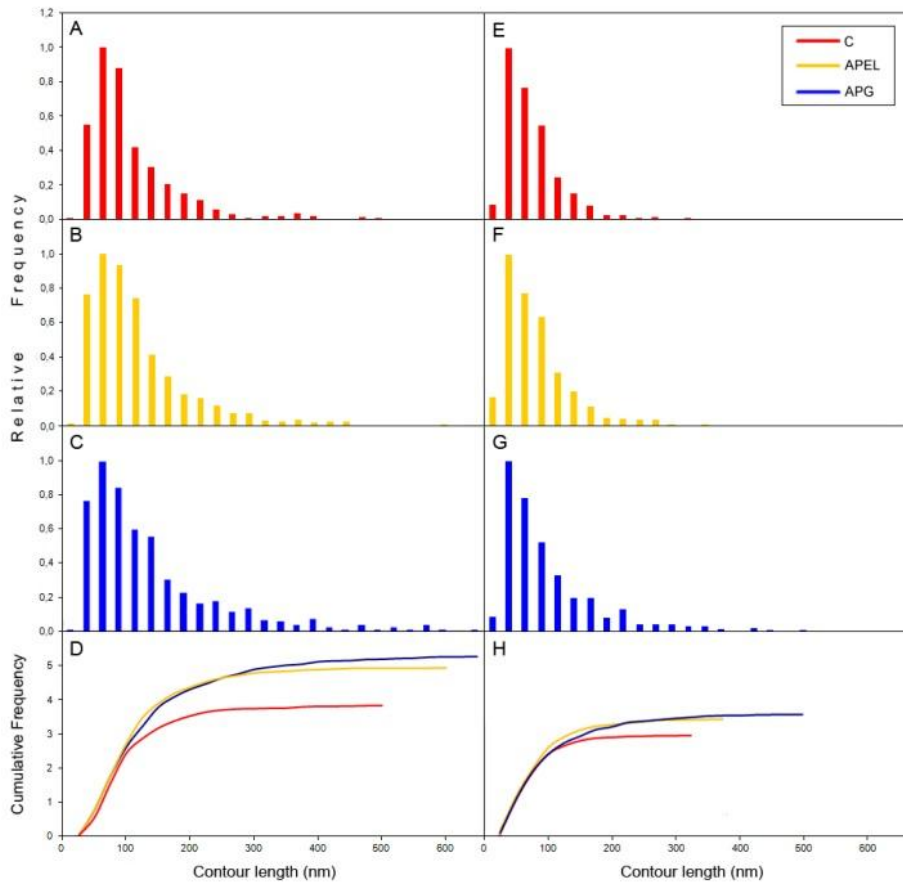


Figure 5. Contour length distribution of CDTA (CSP) and sodium carbonate (SSP) soluble polymers isolated from fruit cell walls of control (A, E), antisense *Fa1C* (APEL; figures B, F) and antisense *FaPG1* (APG; figures C, G) ripe fruits. Bars represent relative frequencies of the observed data. (D, H) Cumulative frequencies for CSP (D) and SSP (H) fractions, normalized to the maximum frequency value.

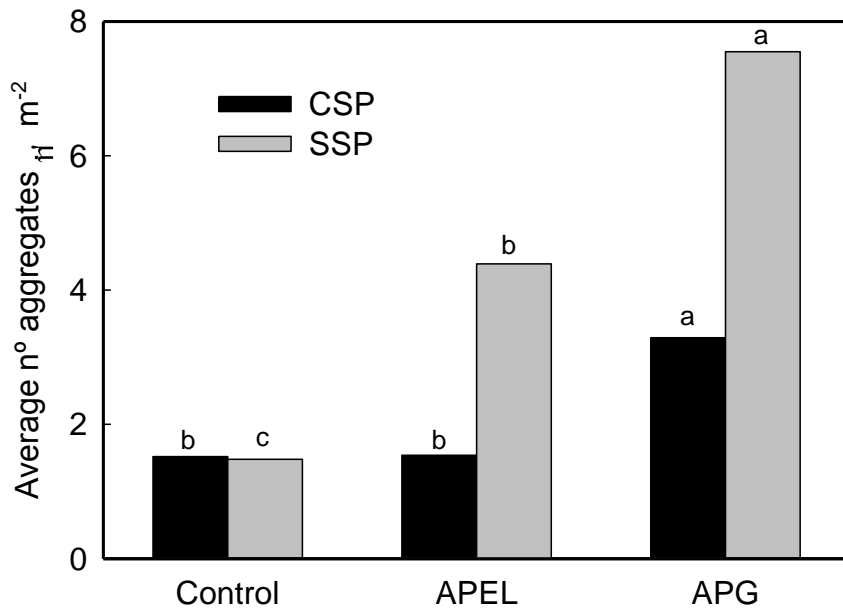


Figure 6. Average number of micellar aggregates in CDTA (CSP) and sodium carbonate (SSP) soluble pectin samples isolated from cell walls of control, antisense *FapIC* (APEL) and antisense *FaPG1* (APG) ripe fruits. For each pectin sample, bars with different letters indicate significant differences by Tukey test at $P=0.05$.

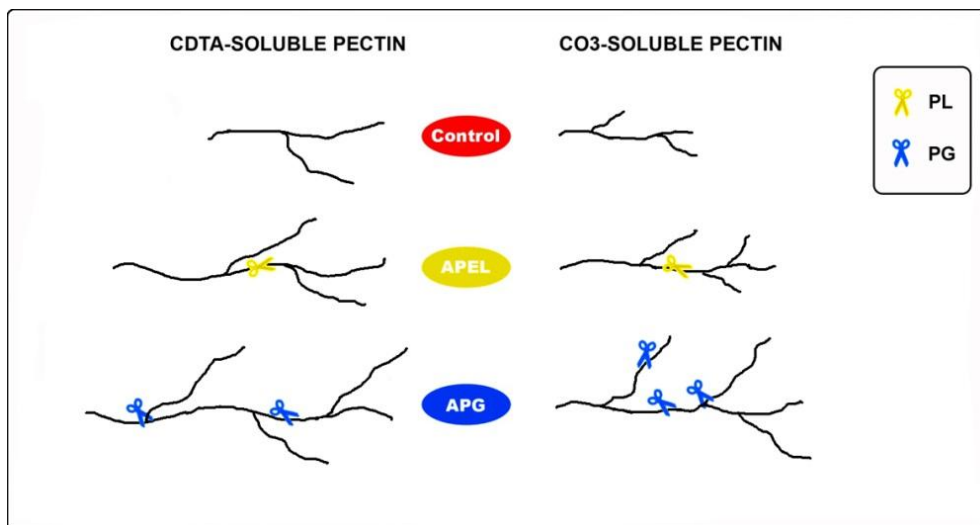


Figure 7. Schematic representation of a hypothetical mode of action for pectate lyase and polygalacturonase on CDTA and sodium carbonate pectin chains during strawberry ripening based on AFM analysis of antisense *FapIC* (APEL) and *FaPG1* (APG) ripe fruits. Length of pectin chains and branches, as well as the number of branches per chain are drawing at scale. Scissors indicate putative points of cutting for both enzymes. Pectate lyase would reduce HGA backbone length and the number of chain branches. This enzyme might play a minor role in the degradation of middle lamella pectins extracted with CDTA. Polygalacturonase has a more pronounced activity during strawberry ripening, degrading HGA backbone, and reducing the number of side-chains of pectins from both polyuronide fractions, as well as the length of sodium carbonate pectin side-chains.

The nanostructural characterization of strawberry pectins in pectate lyase or polygalacturonase silenced fruits elucidates their role in softening

Sara Posé^{a1}, Andrew R. Kirby^b, Candelas Paniagua^a, Keith W. Waldron^b, Victor J. Morris^b, Miguel A. Quesada^c, José A. Mercado^a

^aInstituto de Hortofruticultura Subtropical y Mediterránea “La Mayora” (IHSM-UMA-CSIC), Departamento de Biología Vegetal, Universidad de Málaga, 29071, Málaga, Spain

^bInstitute of Food Research, Norwich Research Park, Colney, Norwich, NR4 7UA, UK

^cDepartamento de Biología Vegetal, Universidad de Málaga, 29071, Málaga, Spain

e-mail: mercado@uma.es

Supplementary Fig. S1. Aspect of plants and fruits from control and antisense *Fa1C* (Apel39) and antisense *FaPG1* (APG29) genotypes.



Supplementary Fig. S2. (A) Representative image of CDTA pectins from strawberry ripe fruit obtained by AFM in contact mode. Branched pectin chains and micellar aggregates with emerging strands can be observed in the image. (B) Height profiles, showing the heights in a true branch point (black arrow) of a polymer chain (profile 1) and micellar aggregates (profile 2) with emerging strands of same height than isolated chains (grey arrow) and higher height at the core area (arrowhead).

